

Supporting Information
for
Reaction of a Nitrosyl Complex of Mn(II)-porphyrinate with Superoxide:
NOD Activity is More Favorable Over SOD Activity

Rakesh Mazumdar, Shankhadeep Saha, Bapan Samanta, Riya Ghosh, Sayani Maity, Biplab Mondal*

Department of Chemistry, Indian Institute of Technology Guwahati, North Guwahati, Assam -781039, India. Phone: +91-361-258-2317; Fax: +91-3612582339. Email: biplab@iitg.ac.in

Table of contents

Sl. No.	Description	Page No.
1	Figure S1. FT-IR spectrum of ligand TMPPH₂ in KBr.	S3
2	Figure S2. ESI-mass spectrum of ligand TMPPH₂ in acetonitrile.	S3
3	Figure S3. ¹ H NMR spectrum of ligand TMPPH₂ in CDCl ₃ .	S4
4	Figure S4. ¹³ C NMR spectrum of ligand TMPPH₂ in CDCl ₃ .	S4
5	Figure S5. FT-IR spectrum of complex 1a in KBr.	S5
6	Figure S6. ESI-mass spectrum of complex 1a in acetonitrile. [Inset: (a) experimental and (b) simulated isotopic distribution pattern].	S5
7	Figure S7. UV-visible spectrum of complex 1a in dichloromethane at RT.	S6
8	Figure S8. X-band EPR spectrum of complex 1a in dichloromethane at 77K.	S6
9	Figure S9. ORTEP diagram of complex 1a (30% thermal ellipsoid plot, H-atoms are omitted for clarity).	S7
10	Figure S10. FT-IR spectrum of complex 1 in KBr.	S7
11	Figure S11. ESI-mass spectrum of complex 1 in acetonitrile. [Inset: (a) experimental and (b) simulated isotopic distribution pattern].	S8
12	Figure S12. UV-visible spectrum of complex 1 in dichloromethane at RT.	S8
13	Figure S13. ¹ H NMR spectrum of complex 1 in DMSO-d ₆ .	S9
14	Figure S14. X-band EPR spectrum of complex 1 in THF at 77K.	S9
15	Figure S15. Cyclic voltammograms of complex 1 in dichloromethane vs. Ag/AgCl, supporting electrolyte 0.1 M TBAP, Scan rate 0.1 v/s.	S10
16	Figure S16: UV-visible spectrum of the reaction mixture of complex 1a and <i>t</i> BuOOH at -40 °C in THF.	S10
17	Figure S17. FT-IR spectrum of complex 2 in KBr.	S11
18	Figure S18. ESI-mass spectrum of complex 2 in acetonitrile. [Inset: (a) experimental and (b) simulated isotopic distribution pattern].	S11
19	Figure S19. UV-visible spectrum of complex 2 in THF.	S12
20	Figure S20. X-band EPR spectrum of complex 2 in THF at 77K.	S12
21	Figure S21. ESI-mass spectrum of 2,4-di- <i>tert</i> -butyl-6-nitrophenol in acetonitrile.	S13
22	Figure S22. ¹ H NMR spectrum of 2,4-di- <i>tert</i> -butyl-6-nitrophenol in CDCl ₃ .	S13

23	Figure S23. ^{13}C NMR spectrum of 2,4-di- <i>tert</i> -butyl-6-nitrophenol in CDCl_3 .	S14
24	Figure S24. ESI-mass spectrum of 9-fluorenone in acetonitrile.	S14
25	Figure S25. ^1H NMR spectrum of 9-fluorenone in CDCl_3 .	S15
26	Figure S26. ^{13}C NMR spectrum of 9-fluorenone in CDCl_3 .	S15
27	Figure S27. ESI-mass spectrum of tmpNO_3 in acetonitrile.	S16
28	Figure S28. ^1H NMR spectrum of tmpNO_3 in CDCl_3 .	S16
29	Figure S29. ^{13}C NMR spectrum of $(\text{tmp})(\text{NO}_3)$ in CDCl_3 .	S17
30	Figure S30. ORTEP diagram of tmpNO_3 (30% thermal ellipsoid plot, H-atoms are omitted for clarity).	S17
31	Table S1. Crystallographic data for complex 2 .	S18
32	Table S2. Selected bond lengths (\AA) of complex 2 .	S18
33	Table S3. Selected bond angles ($^\circ$) of complex 2 .	S19

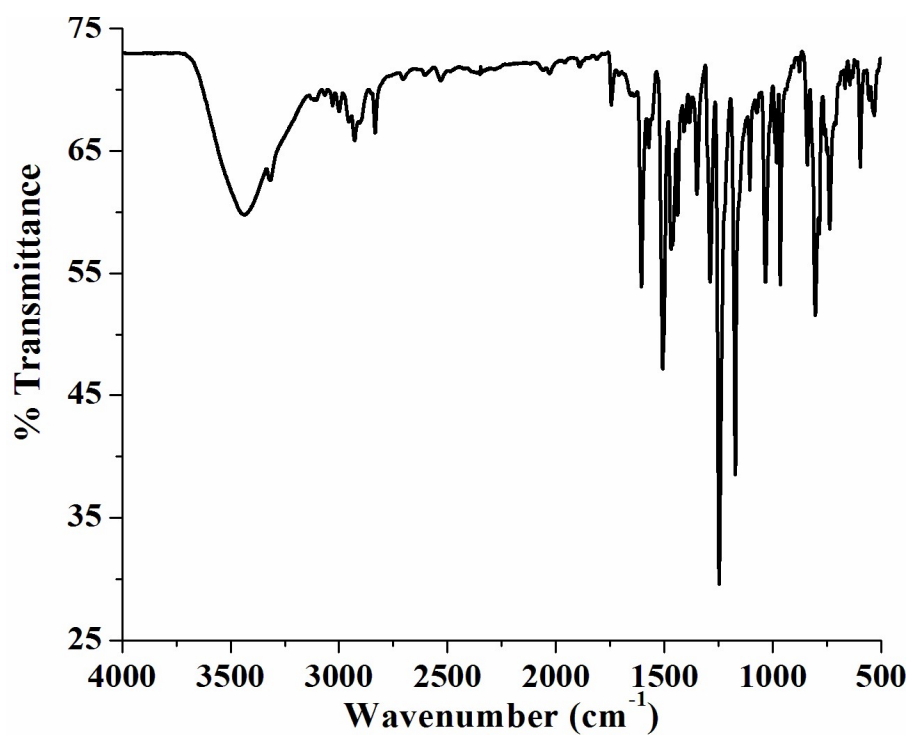


Figure S1. FT-IR spectrum of ligand TMPPH_2 in KBr.

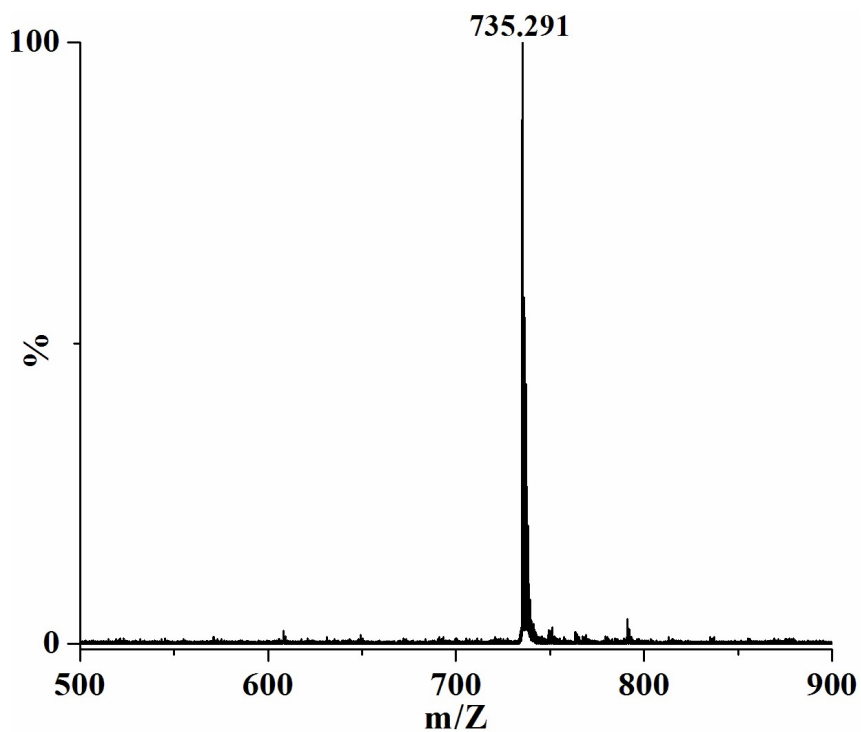


Figure S2. ESI-mass spectrum of ligand TMPPH_2 in acetonitrile.

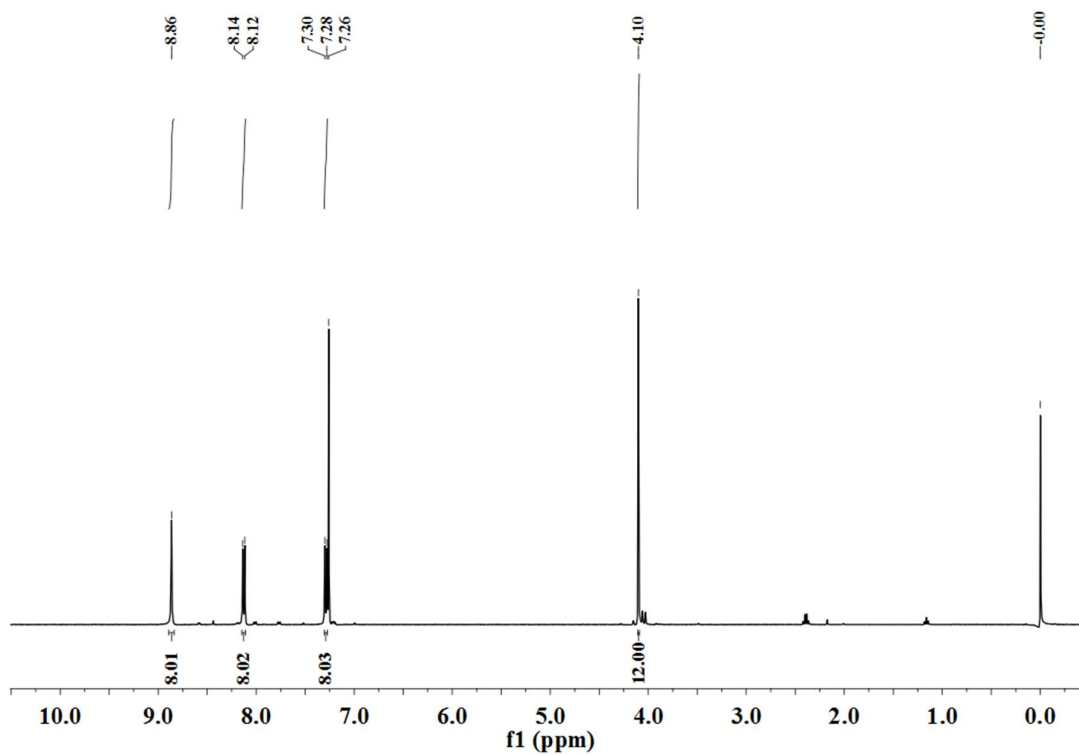


Figure S3. ^1H NMR spectrum of ligand TMPPH_2 in CDCl_3 .

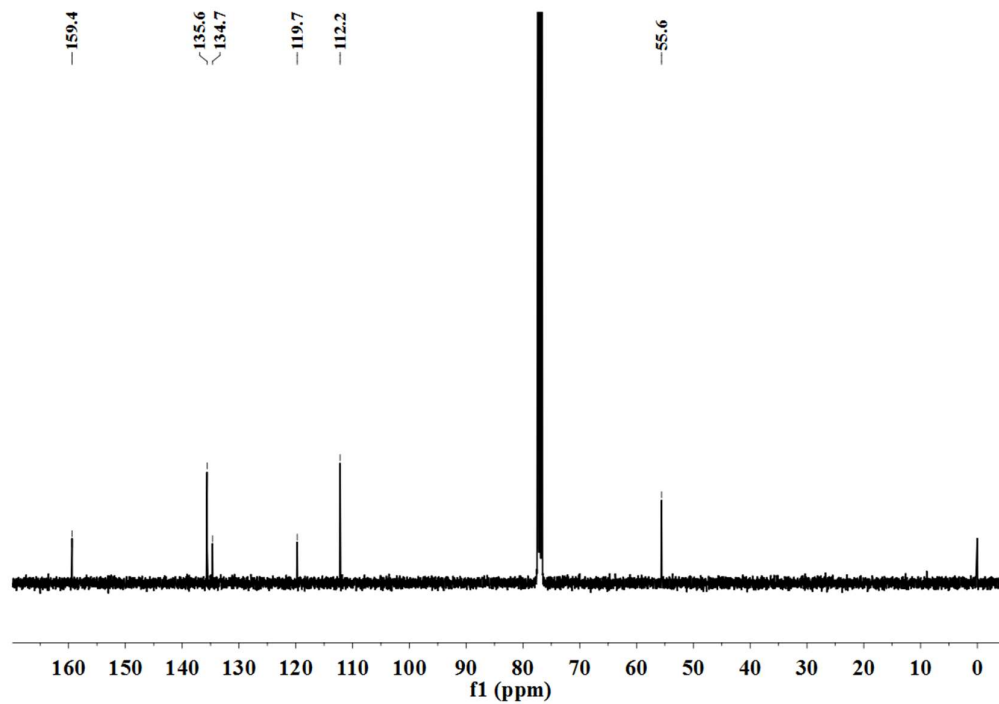


Figure S4. ^{13}C NMR spectrum of ligand TMPPH_2 in CDCl_3 .

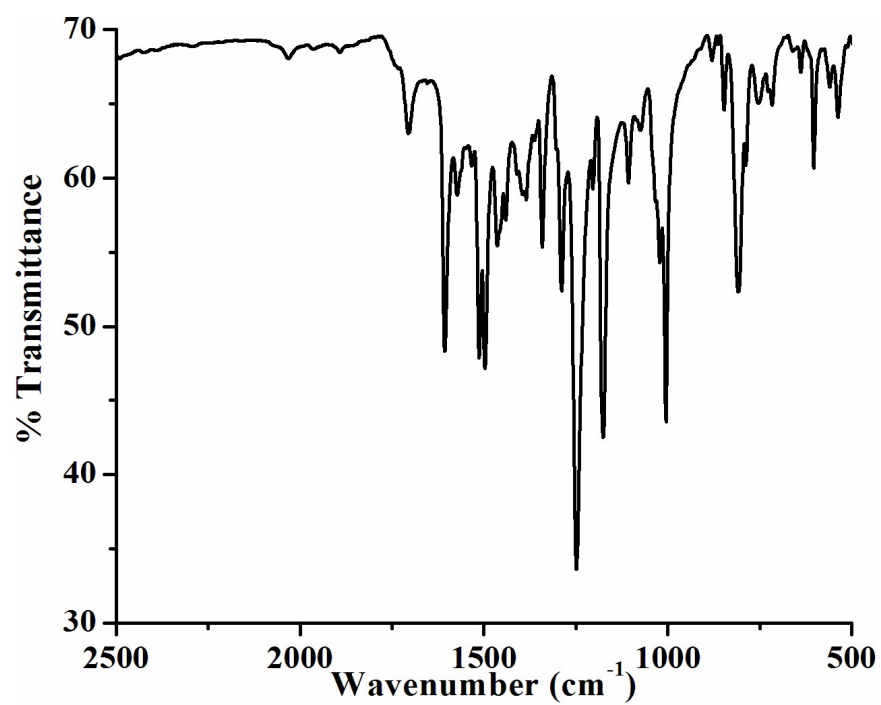


Figure S5. FT-IR spectrum of complex **1a** in KBr.

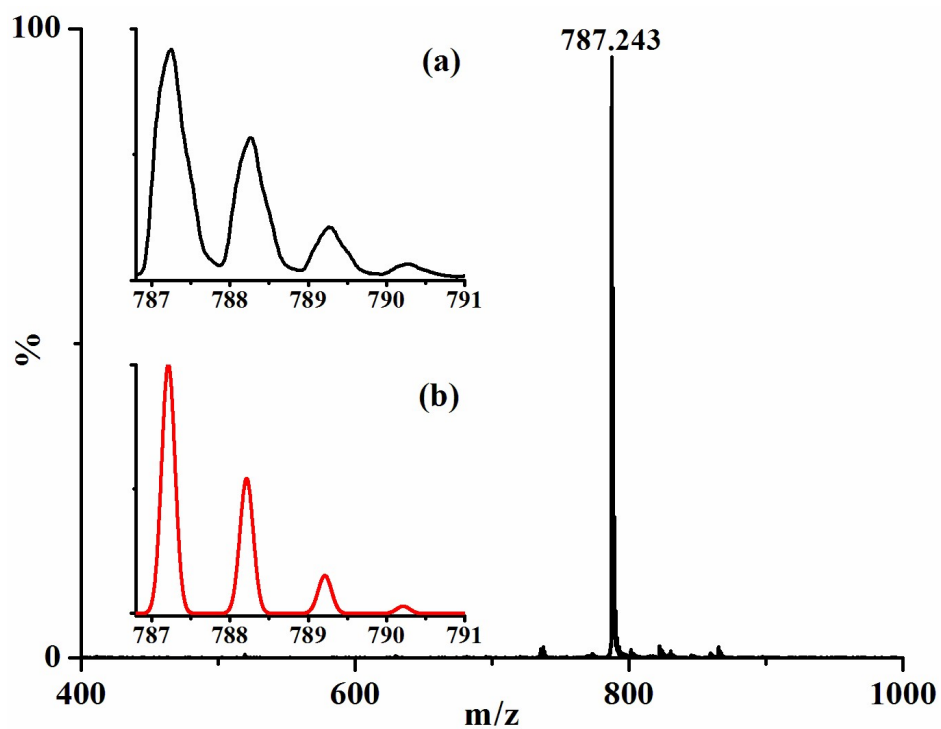


Figure S6. ESI-mass spectrum of complex **1a** in acetonitrile. [Inset: (a) experimental and (b) simulated isotopic distribution pattern].

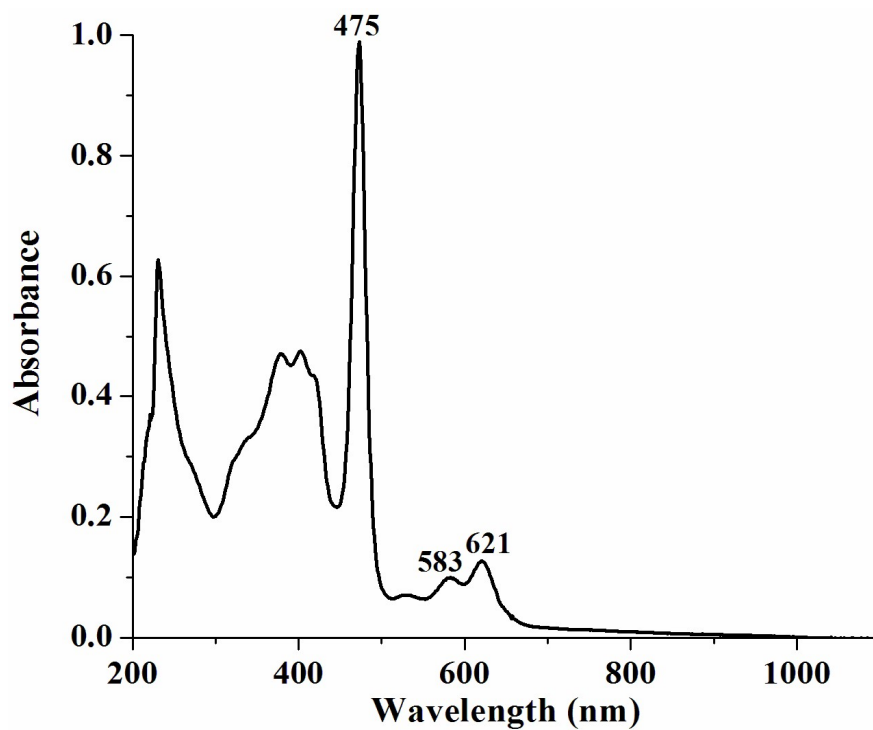


Figure S7. UV-visible spectrum of complex **1a** in dichloromethane at RT.

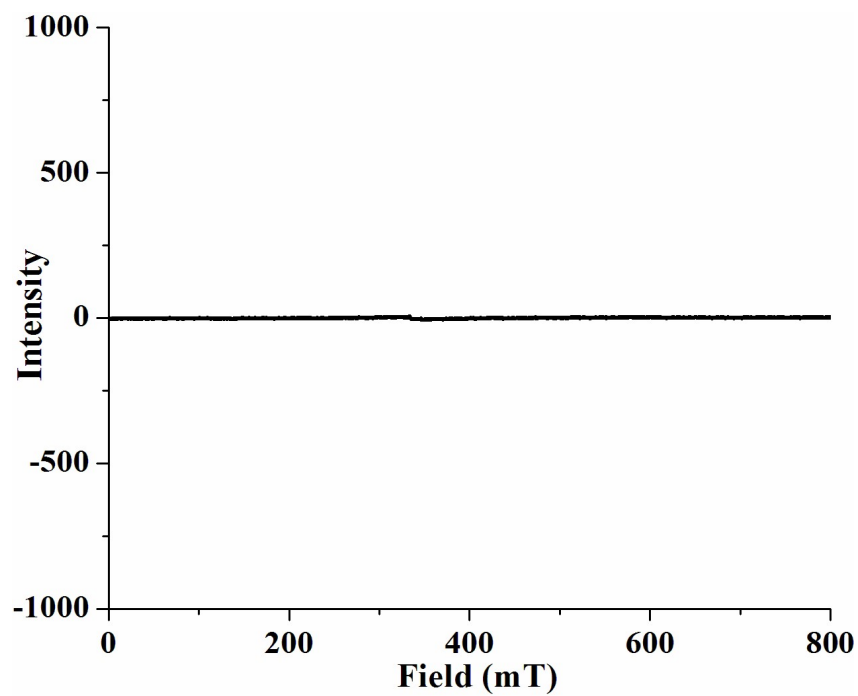


Figure S8. X-band EPR spectrum of complex **1a** in dichloromethane at 77K.

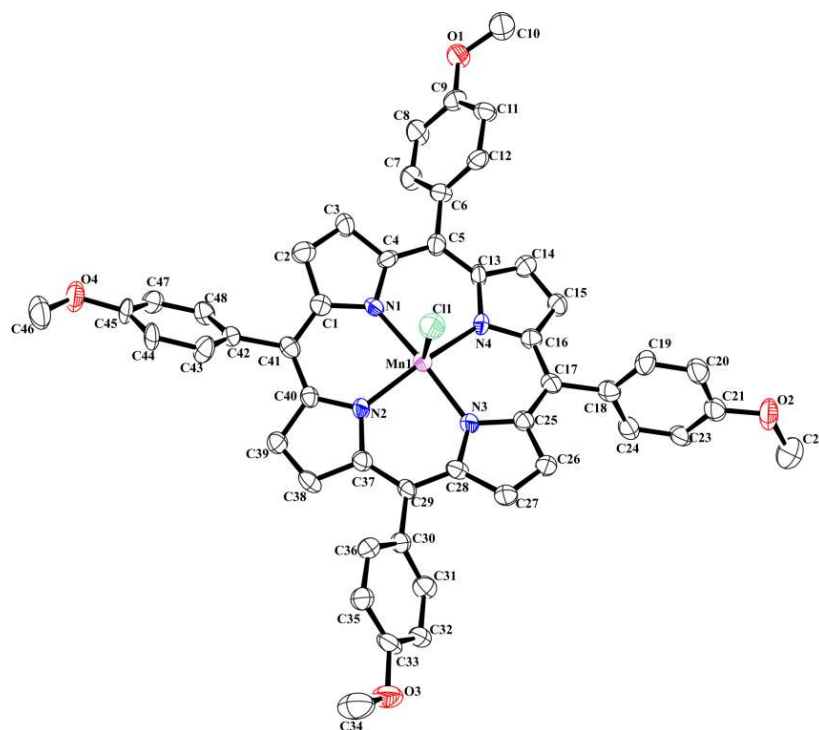


Figure S9. ORTEP diagram of complex **1a** (30% thermal ellipsoid plot, H-atoms are omitted for clarity).

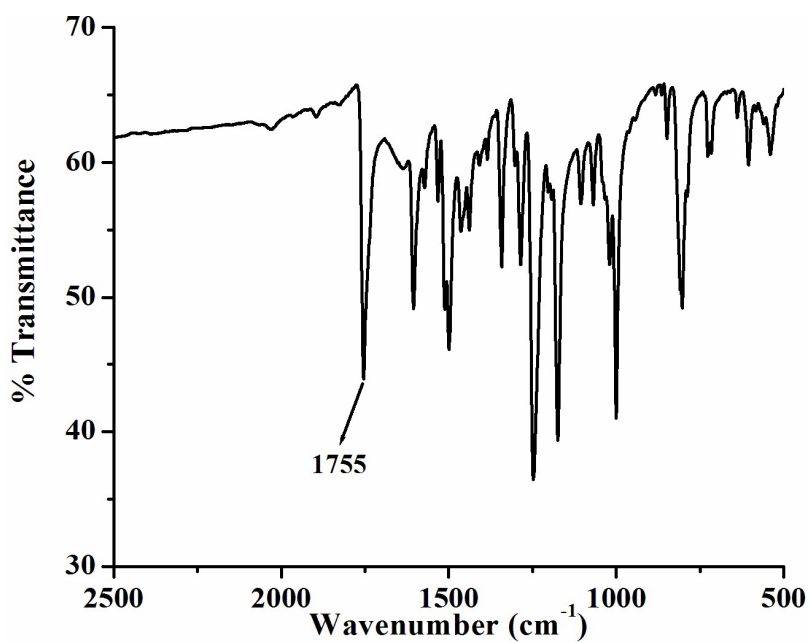


Figure S10. FT-IR spectrum of complex **1** in KBr.

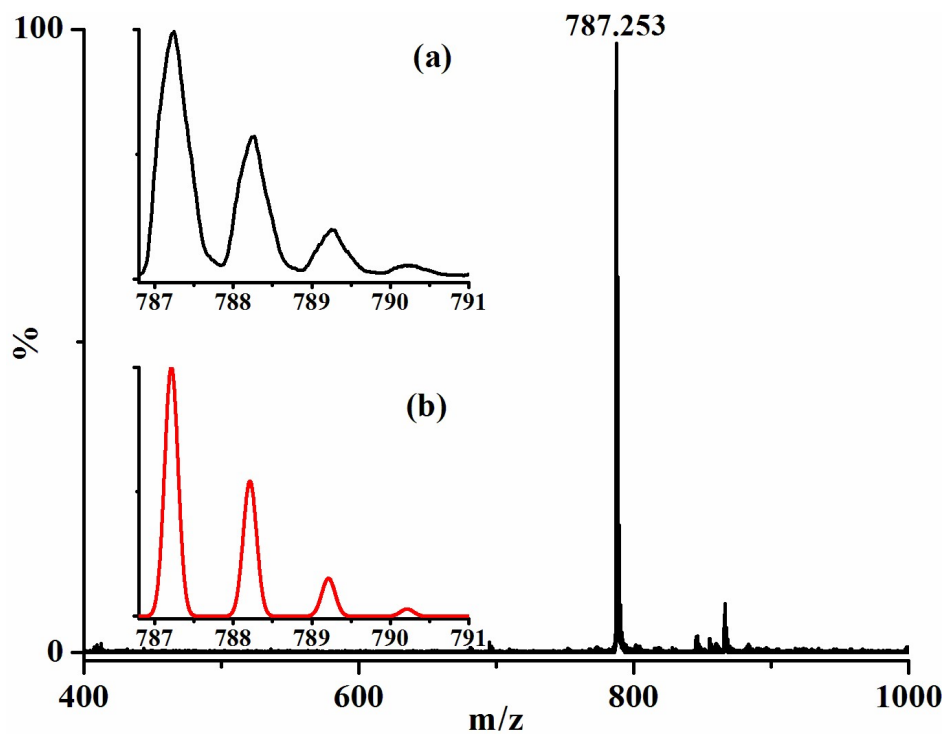


Figure S11. ESI-mass spectrum of complex 1 in acetonitrile. [Inset: (a) experimental and (b) simulated isotopic distribution pattern].

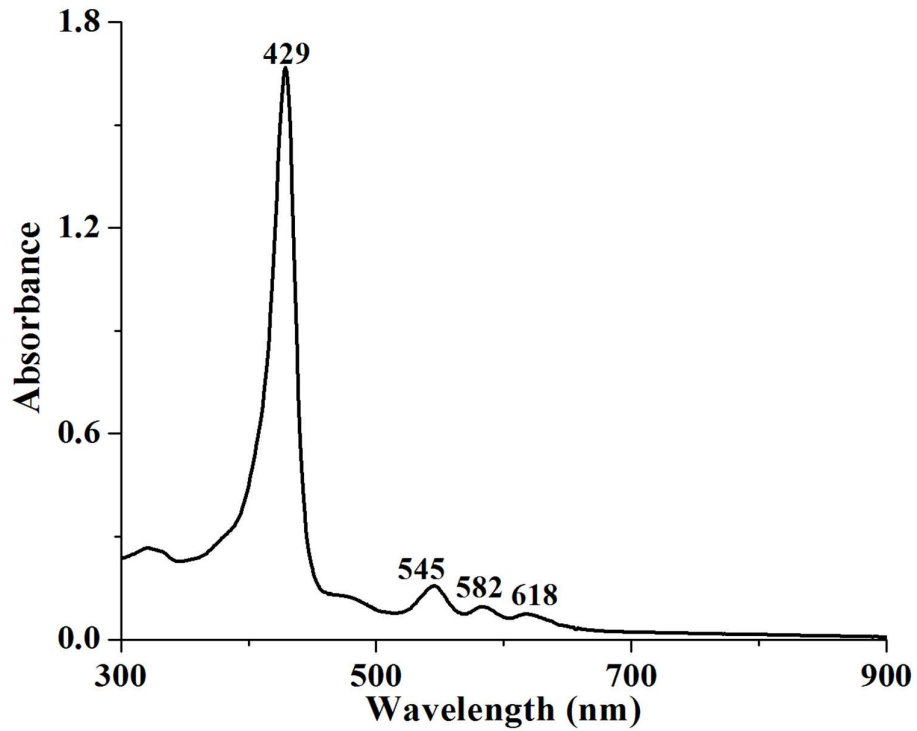


Figure S12. UV-visible spectrum of complex 1 in dichloromethane at RT.

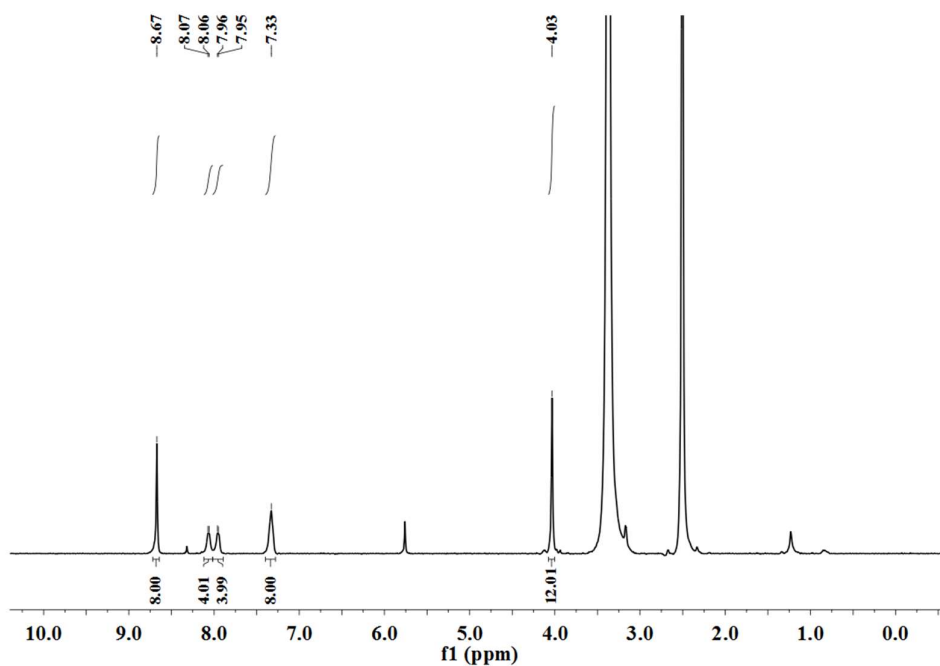


Figure S13. ¹H NMR spectrum of complex 1 in DMSO-d₆.

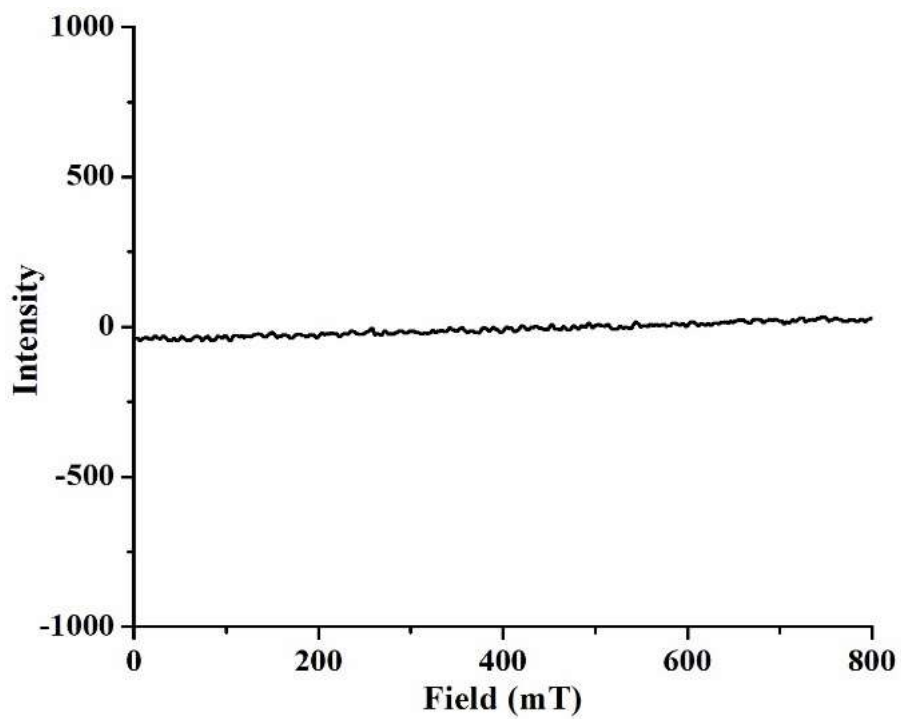


Figure S14. X-band EPR spectrum of complex 1 in THF at 77K.

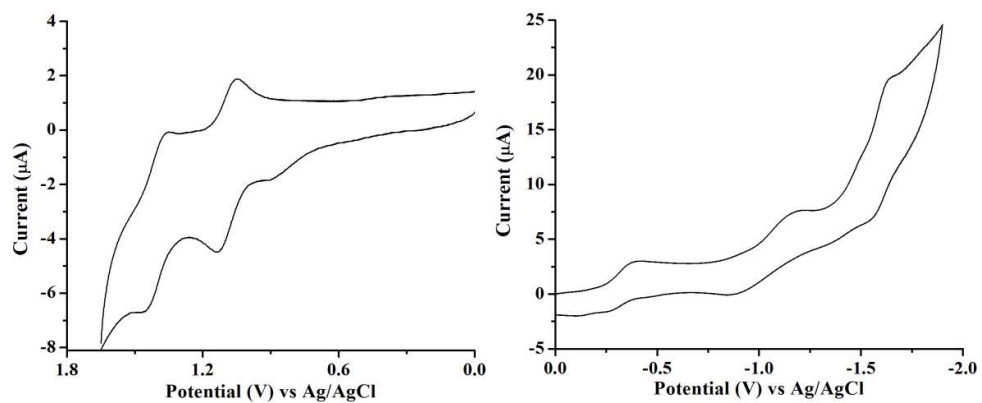


Figure S15. Cyclic voltammograms of complex **1** in dichloromethane vs. Ag/AgCl, supporting electrolyte 0.1 M TBAP, Scan rate 0.1 v/s.

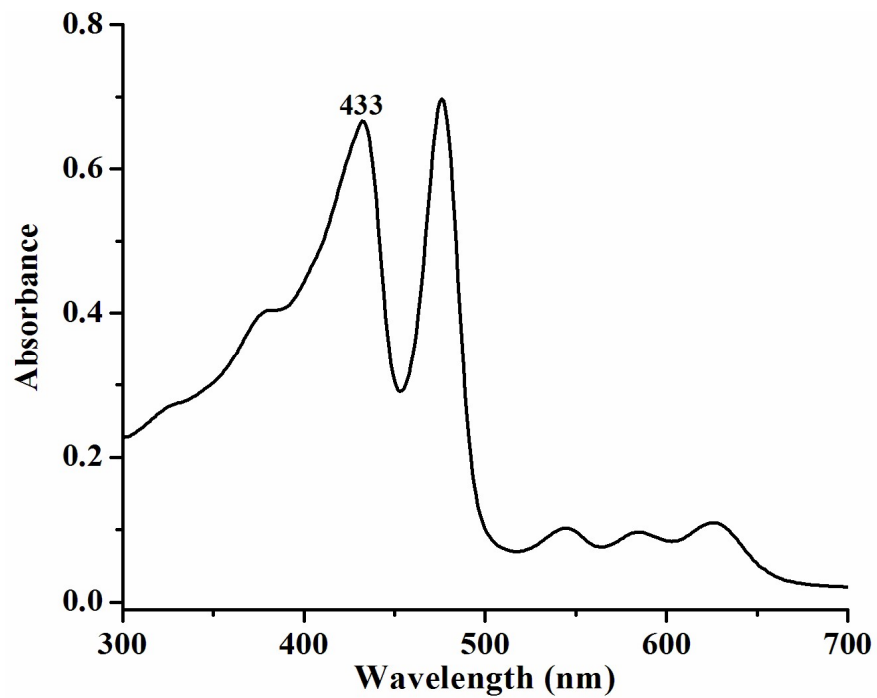


Figure S16: UV-visible spectrum of the reaction mixture of complex **1a** and *t*BuOOH at $-40\text{ }^{\circ}\text{C}$ in THF.

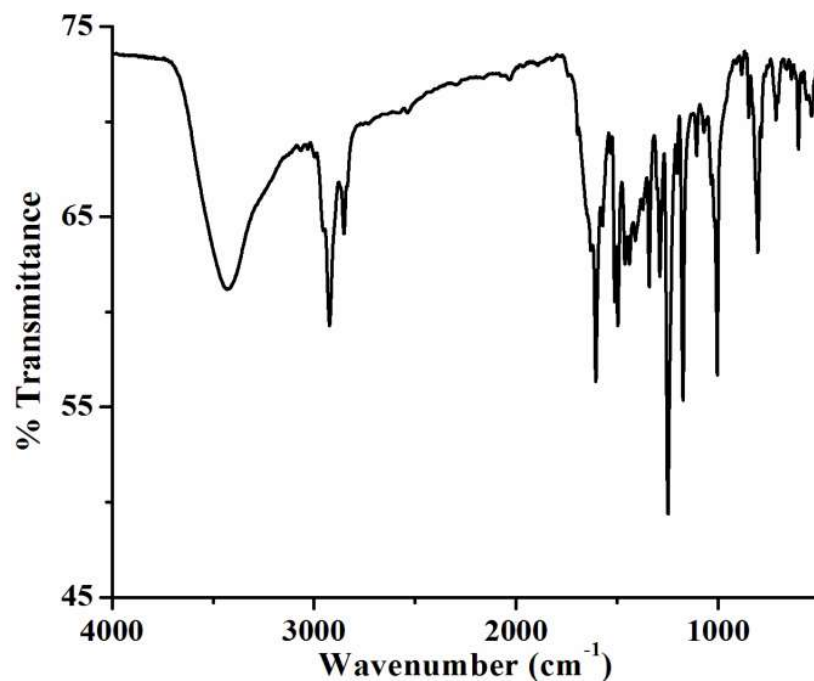


Figure S17. FT-IR spectrum of complex **2** in KBr.

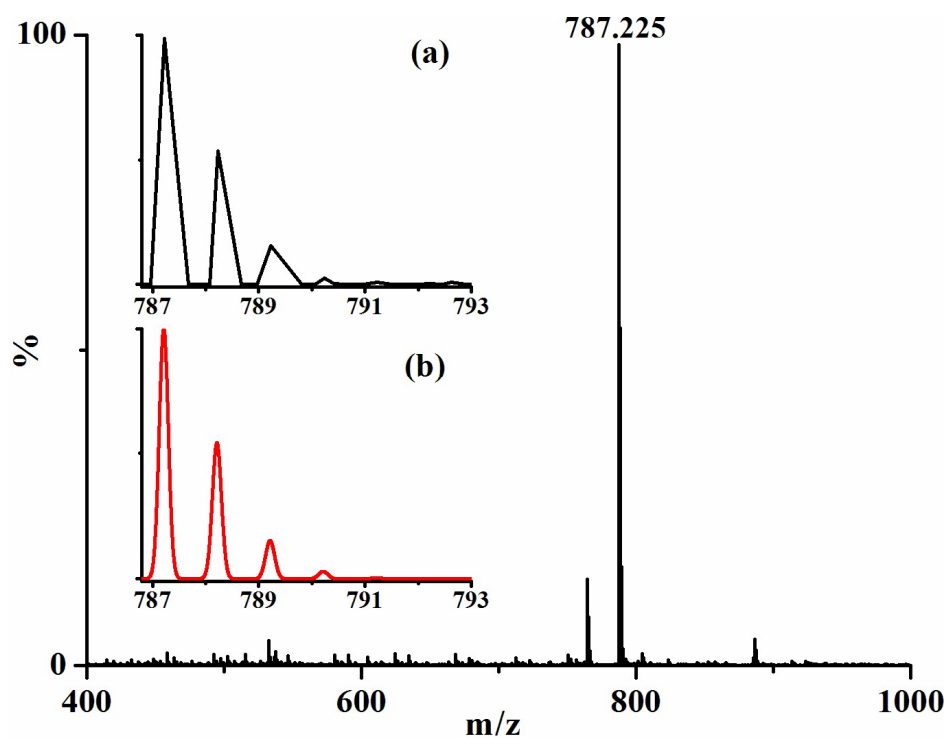


Figure S18. ESI-mass spectrum of complex **2** in acetonitrile. [Inset: (a) experimental and (b) simulated isotopic distribution pattern].

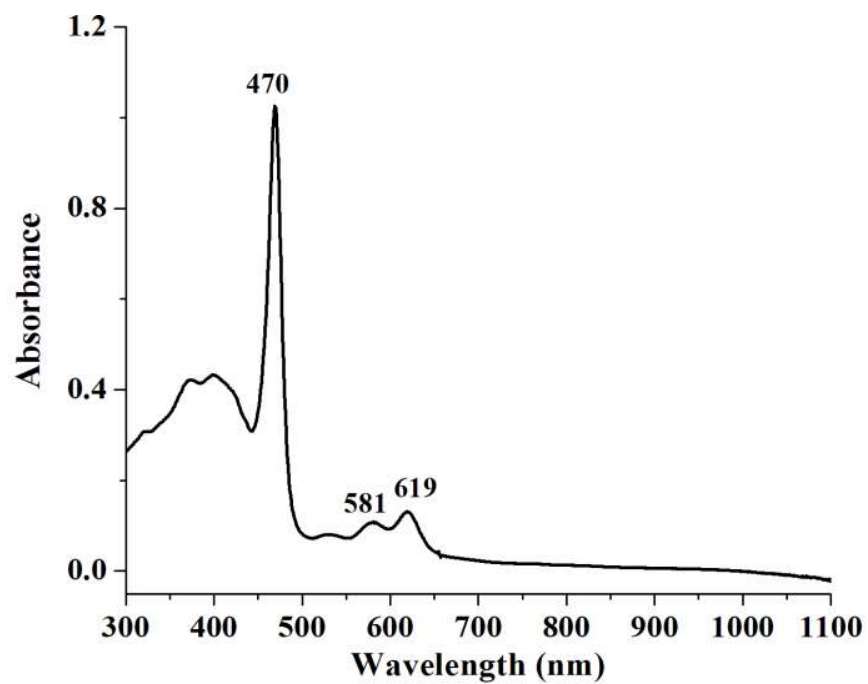


Figure S19. UV-visible spectrum of complex 2 in THF.

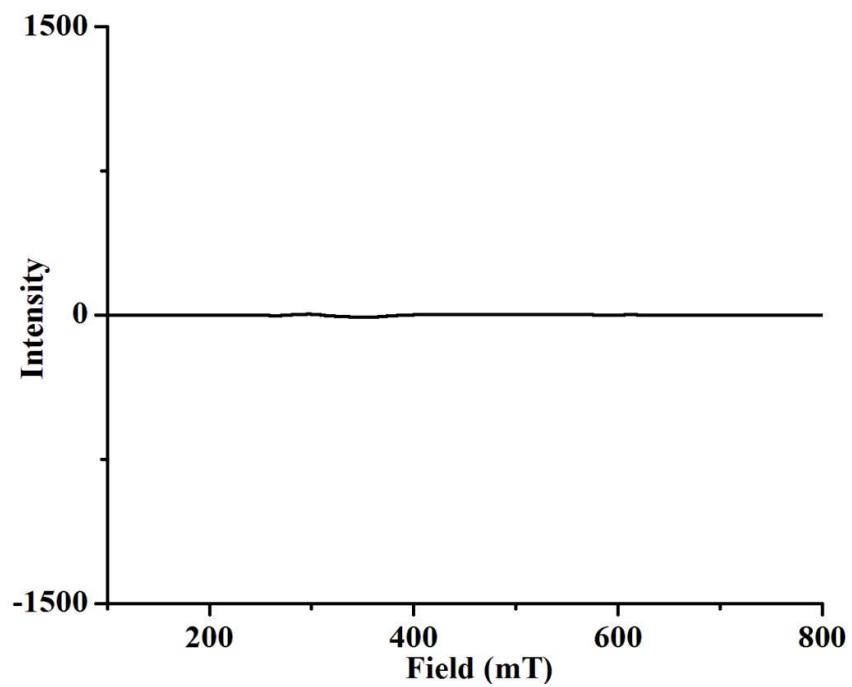


Figure S20. X-band EPR spectrum of complex 2 in THF at 77K.

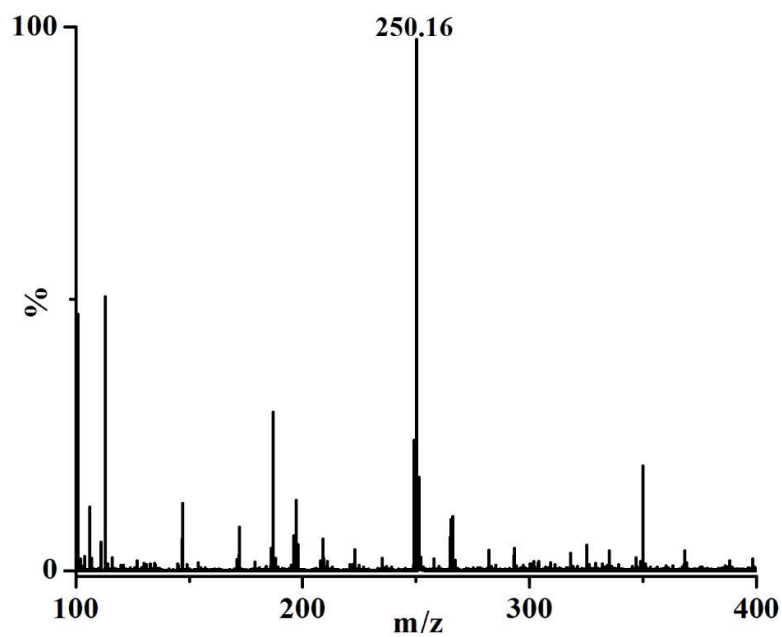


Figure S21. ESI-mass spectrum of 2,4-di-*tert*-butyl-6-nitrophenol in acetonitrile.

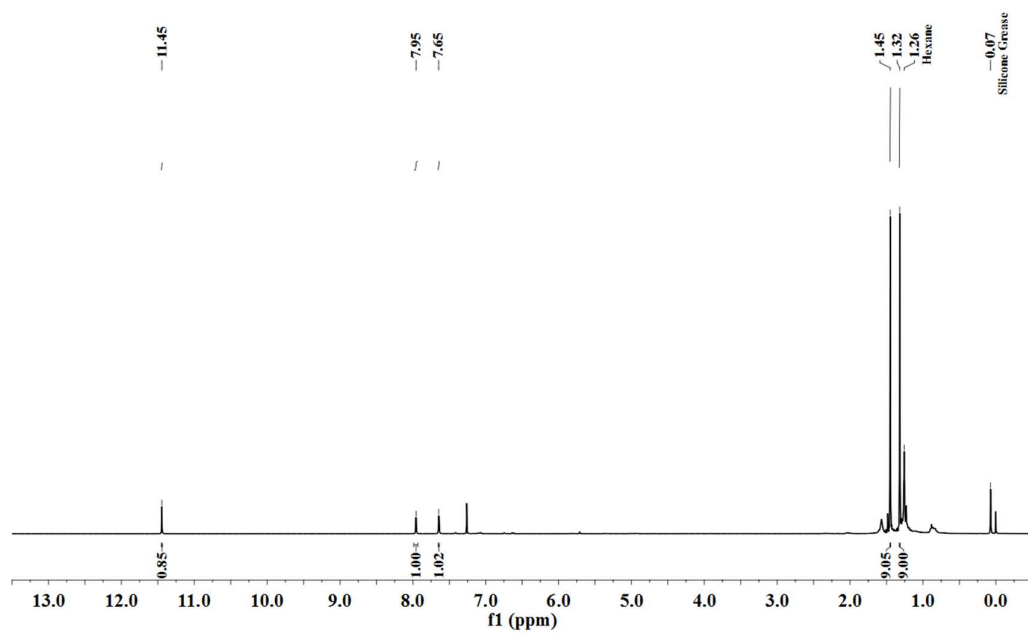


Figure S22. ¹H NMR spectrum of 2,4-di-*tert*-butyl-6-nitrophenol in CDCl₃.

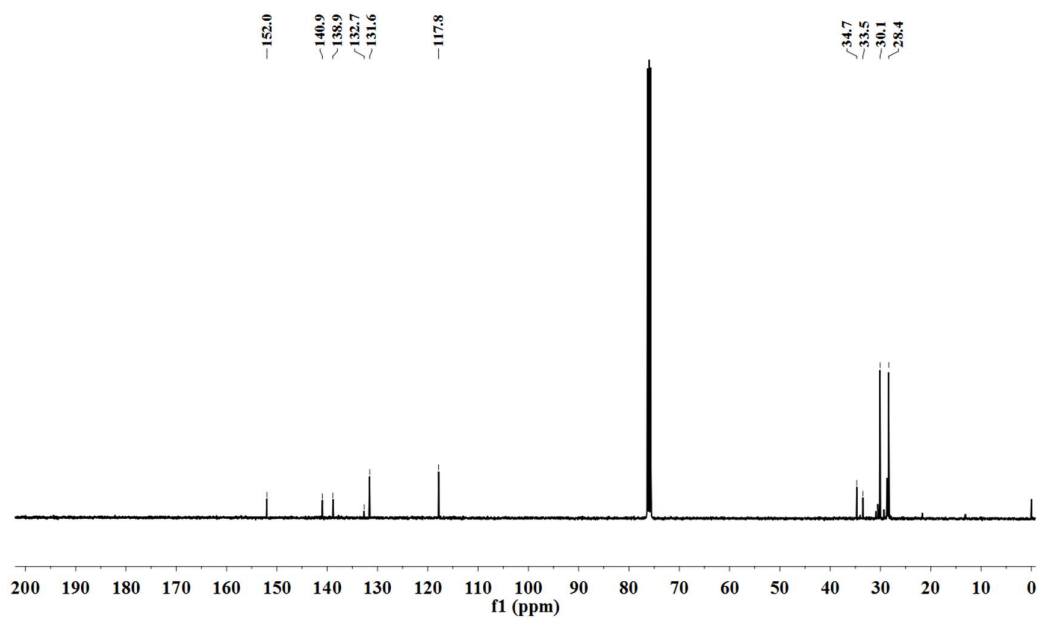


Figure S23. ^{13}C NMR spectrum of 2,4-di-*tert*-butyl-6-nitrophenol in CDCl_3 .

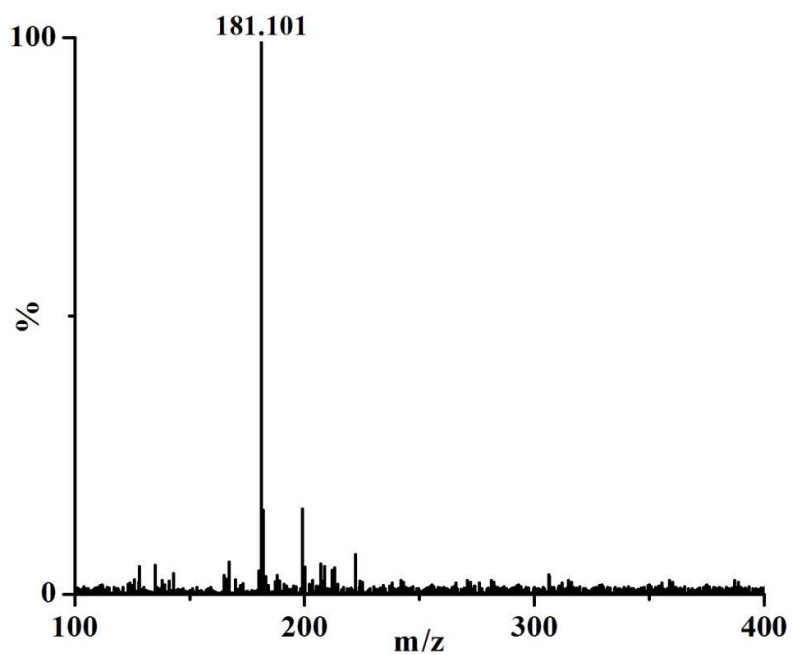


Figure S24. ESI-mass spectrum of 9-fluorenone in acetonitrile.

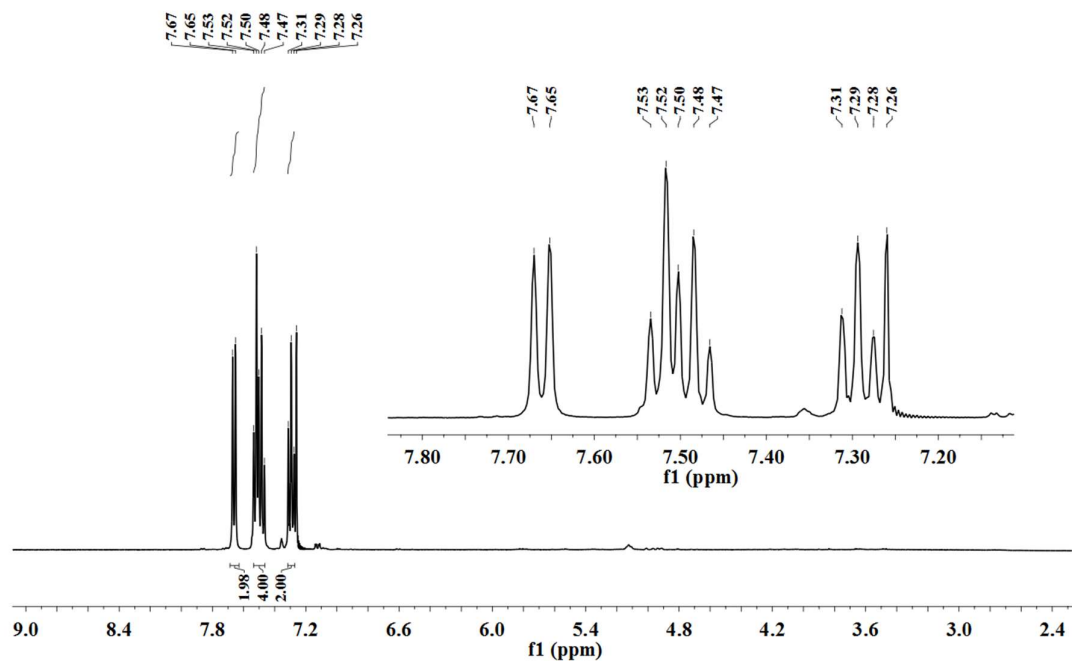


Figure S25. ^1H NMR spectrum of 9-fluorenone in CDCl_3 .

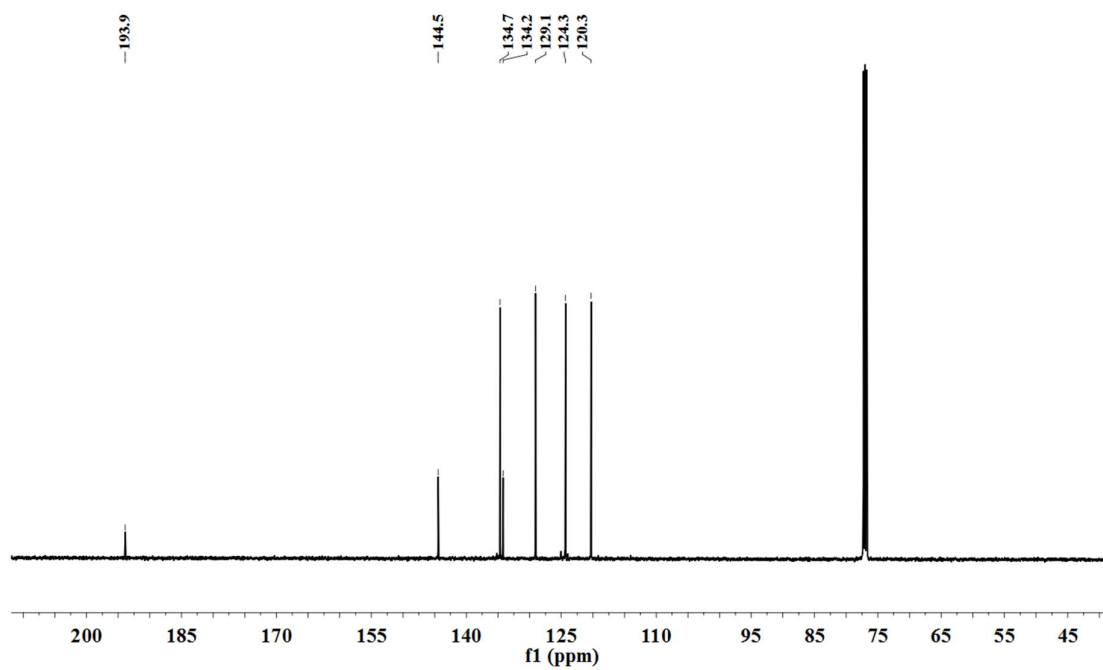


Figure S26. ^{13}C NMR spectrum of 9-fluorenone in CDCl_3 .

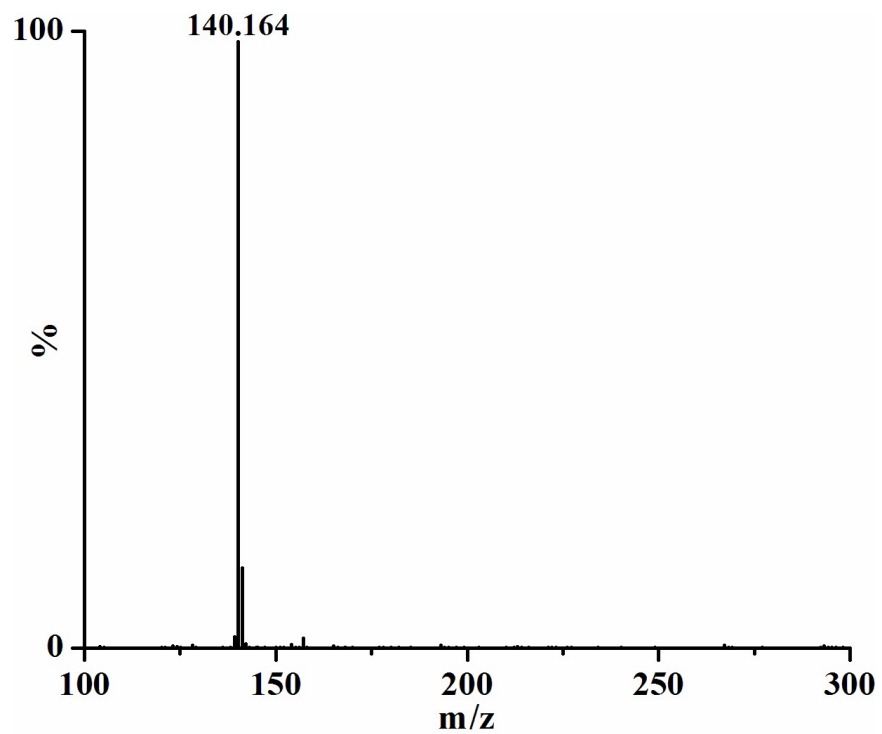


Figure S27. ESI-mass spectrum of tmpNO₃ in acetonitrile.

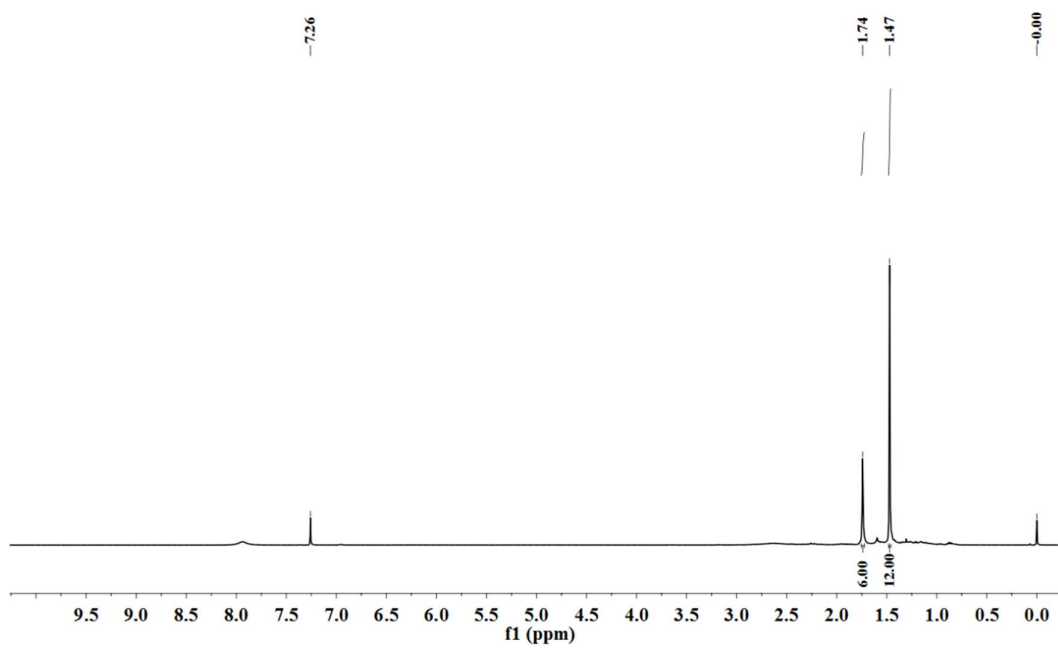


Figure S28. ¹H NMR spectrum of tmpNO₃ in CDCl₃.

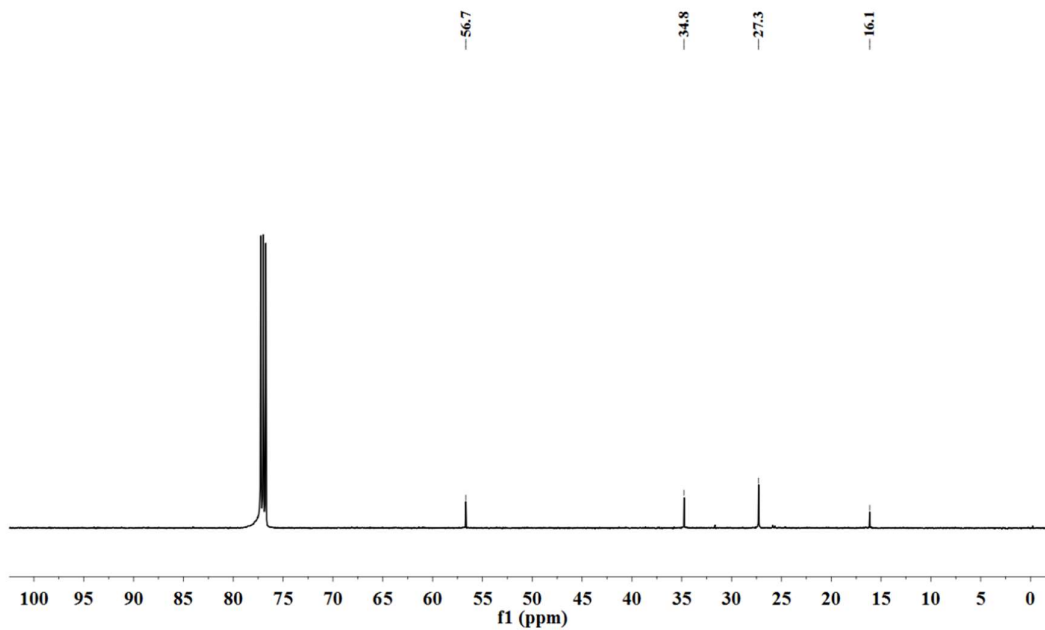


Figure S29. ^{13}C NMR spectrum of tmpNO₃ in CDCl₃.

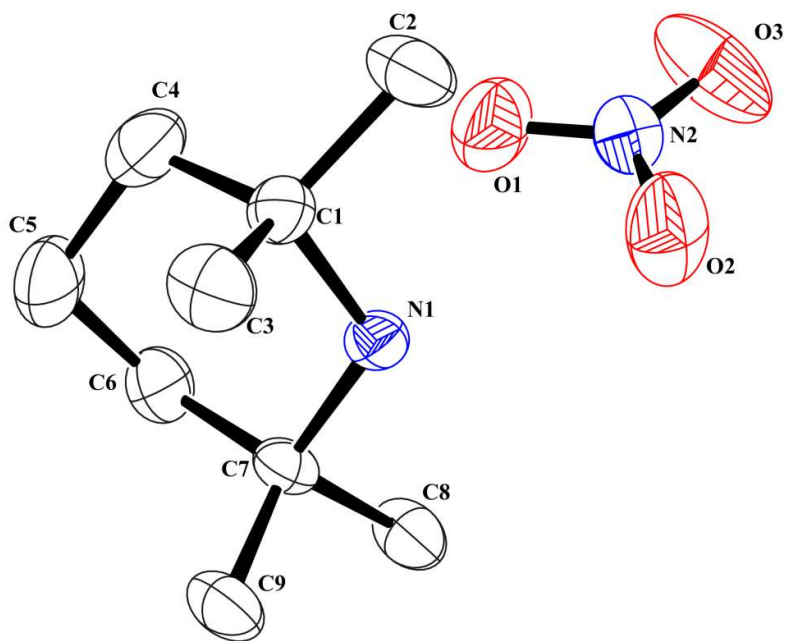


Figure S30. ORTEP diagram of tmpNO₃ (30% thermal ellipsoid plot, H-atoms are omitted for clarity).

Table S1. Crystallographic data for complex **2**.

	2
Formulae	C ₄₈ H ₃₈ N ₄ O ₆ Mn
Mol. wt.	821.76
Crystal system	Monoclinic
Space group	P 21/c
Temperature /K	100(2)
Wavelength /Å	0.71073
<i>a</i> /Å	9.8(2)
<i>b</i> /Å	10.4(2)
<i>c</i> /Å	21.2(4)
α /°	90
β /°	111.6(7)
γ /°	90
V/ Å ³	2009(68)
Z	2
Density/Mgm ⁻³	1.358
Abs. Coeff. /mm ⁻¹	0.385
Abs. correction	none
F(000)	854
Total no. of reflections	3524
Reflections, $I > 2\sigma(I)$	1310
Max. 2θ /°	24.995
Ranges (h, k, l)	-11 ≤ h ≤ 11 -12 ≤ k ≤ 12 -11 ≤ l ≤ 25
Complete to 2θ (%)	0.998
Refinement method	Full-matrix least-squares on F^2
Goof (F^2)	0.841
R indices [$I > 2\sigma(I)$]	0.0904
R indices (all data)	0.1702

Table S2. Selected bond lengths (Å) of complex **2**.

Atoms	2
Mn1-N1	1.91(3)
Mn1-N2	1.95(3)
Mn1-O1	2.13(3)
C1-C2	1.28(2)
C2-C3	1.37(3)
C4-C5	1.49(2)
C5-C6	1.32(2)
C6-C7	1.37(2)

Table S3. Selected bond angles (°) of complex **2**.

Atoms	2
N1-Mn1-N2	86.8(12)
N1-Mn1-O1	90.5(14)
C1-C2-C3	105.2(11)
C5-C6-C7	119.3(14)
C8-O2-C9	119.8(7)